RSC Advances

Polymeric Foams with Functional Nanocomposite Cells

Journal:	*RSC Advances*
Manuscript ID:	RA-ART-01-2014-000823.R1
Article Type:	Paper
Date Submitted by the Author:	19-Mar-2014
Complete List of Authors:	Calcagnile, Paola; IIT, Fragouli, Despina; Italian Institute of Technology, Center for biomolecular nanotechnologies Mele, Elisa; Center for Biomolecular Nanotechnologies, Istituto Italiano di Tecnologia Ruffilli, Roberta; Istituto Italiano di Tecnologia, I.I.T., Athanassiou, Athanassia; Italian Institute of Technology, ;

Journal Name

RSCPublishing

ARTICLE

Polymeric Foams with Functional Nanocomposite Cells

Cite this: DOI: 10.1039/x0xx00000x

P. Calcagnile,[a] D. Fragouli,[*b] E. Mele,[b] R. Ruffilli,[c] and A. Athanassiou[b]

Received 00th January 2012,
Accepted 00th January 2012

DOI: 10.1039/x0xx00000x

www.rsc.org/

A novel strategy for the fabrication of elastomeric poly(dimethylsiloxane) (PDMS) foams with interconnected nanocomposite cells of controlled size is presented. Beads of the natural hydrogel calcium alginate, are used as templates for the fabrication of the foams and as initiators for the functionalization of their cells with gold nanoparticles. The hydrogel beads are easily fabricated via external gelation using a fluidic system that permits the control of their size. As a subsequent step, they are closely assembled in containers where PDMS pre-polymer is poured. As the elastomer cures, the beads shrink releasing the liquid they contain and forming pores in the polymer matrix. By introducing gold precursor solution in the beads, it is possible to develop foams with gold nanoparticles immobilized on the surface of their cells. As the gold ions solution is released by the beads, it chemically interacts with the PDMS, forming nanoparticles locally onto the surface of the cavities of the foams. The same procedure can be expanded to various substances resulting in functional foams with localized properties, envisaging applications in the biomedical field.

Introduction

Polymeric foams are porous materials composed by gaseous voids surrounded by a polymer matrix. They are of great interest since they merge the advantages of polymeric materials, such as low cost, diversity of mechanical properties and high processability, with those of porous materials, such as high surface area, sound and thermal isolation, light weight, etc. They have been widely used in countless applications including scaffolds,[1] filtration/separation,[2] shock and sound attenuation.[3] Typical porous structures can be obtained by different strategies, as gas-foaming methods using supercritical fluids[4] or other blowing agents,[5,6] freeze-drying,[7] solvent casting and particulate leaching,[8-13] high internal phase emulsions (HIPEs),[14, 15] fiber felt or meshes,[16, 17, 18] electrospinning[19] or bijel templates.[20]

The majority of these methods presents diverse drawbacks as they often employ harmful agents and consume high amounts of energy. Moreover, the resulting foams have not defined and controlled pore size and structure but rather a broad macropore-size distribution with mixed open and closed cells. Most importantly, in polymeric nanocomposite foams the homogenous distribution of nanofillers requires complicated and time consuming methods[21]. In most cases, the nanoparticles are distributed in the whole volume of the polymer, and no particular attention is paid on the localized physicochemical properties of the surface of the pores (chemistry, roughness, etc.). This may induce limitations for applications were the surface functionality of the pores is important (e.g. biological and chemical reactions). So far, no study has been presented on foams characterized by the localization of the fillers exclusively on the cells' surface. Such process could pave the way to the utilization of functional foams with nanocomposite cells, as scaffolds for localized cells growth, matrices for localized molecular detection or reactions, or as systems with multifunctional properties.

Targeting these applications, a facile and eco-friendly alternative to the current methods for the fabrication of flexible polymeric foams with controlled pores' size and, most importantly, chemical composition is presented herein. A direct templating technique is exploited, based on the close packing and subsequent shrinking of monodispersed hydrogel beads of calcium alginate into a matrix of poly(dimethylsiloxane) (PDMS). When the polymer is completely cured and the beads are dried, the latter are removed from the polymeric matrix upon mechanical pressure applied by water flow. This results in the formation of elastomeric foams with well-defined pores. Above all, the proposed method is suitable for fabrication of multifunctional foams, where the functional substances/fillers are exclusively localized onto the surface of the cells. This is succeeded by taking advantage of the ability of the hydrogel beads to encapsulate and subsequent release, during shrinking, various nanoparticle (NP) precursors or active macromolecules[22, 23]. As a proof of concept, gold (Au) metal precursor is encapsulated in the beads and its chemical

reduction, due to the interaction with the PDMS polymeric matrix, results in the formation of Au NPs. Thus, using a two-step method (encapsulation and shrinking/release) polymeric foams with nanocomposite cells can be fabricated. To the best of our knowledge only few studies have employed hydrogel beads as templates in order to fabricate purely polymeric foams[24-27]. In these works, the utilization of acidic or sodium citrate solutions for the leaching of the beads from the polymeric foam matrices presents serious drawbacks due to possible acid residuals remaining into the structure. So far, no study on foams took advantage of the natural shrinking or the encapsulation and release properties of the alginate beads. These processes permit their facile removal from the elastomeric matrix without any chemical treatment of the foams and the functionalization of the surface of the formed pores.

Experimental

Materials

Powder of alginic acid sodium salt, anhydrous granular calcium chloride, and gold (III) chloride trihydrate ($HAuCl_4$) were purchased from Sigma-Aldrich and used without further purification. Poly(dimethylsiloxane) (PDMS) supplied in two compounds: monomer and curing agent (Sylgard 184 Silicone Elastomer) was purchased from Dow Corning Corporation. Sunflower seed oil (De Santis) and a detergent (Ausilab, Carlo Erba) where utilized for the fabrication of sub-millimeter sodium alginate beads with a fluidic system. All aqueous solutions were prepared with purified water through a Milli-Q Plus system.

Fabrication Method of Beads and Fluidics Setup

Calcium alginate beads of millimetric size (diameter D_1 = 1.56 ± 0.06 mm) were prepared by dropwise addition of 3%wt of sodium alginate aqueous solution in a calcium chloride one (7%wt) through a syringe (2.5 ml volume) with a stainless steel 30 gauge needle. The solution was injected by a syringe pump (New Era Pump System Inc.) using a stable flow rate (r_s) of 0.05 ml/min. Sub-millimetric beads were formed using a system consisting of two fluidic ports connected to form a T-junction. Sunflower seed oil from the first and the sodium alginate aqueous solution from the second port were injected with stable flow rates into a plastic capillary tube (Tygon, internal diameter of 1.6 mm) (Supplementary Information, Fig. S1). The flow rate of the sodium alginate solution (r_s) was interrupted by the continuous flow of oil at higher rate (r_o), creating spheres of sodium alginate with controlled size into the oil capillary tube. The as created spheres were dropped in a bath containing 7%wt concentrated aqueous solution of calcium chloride, where they underwent external gelation due to the presence of calcium ions, forming thus calcium alginate beads. In order to prevent the coalescence of the sodium alginate spheres, a surfactant (detergent) was previously added into the calcium chloride solution[28, 29].

In the case of the formation of calcium alginate beads containing gold precursor, the sodium alginate spheres were crosslinked in an aqueous solution of 10%wt calcium chloride and 0.1%wt $HAuCl_4$ with respect to the water. The beads obtained in such way, differently from the simple calcium alginate ones, are kept in the calcium ions solution for 1 week and, like the others, carefully washed in distilled water before being used as templates for the formation of the foam. By adjusting the flow rates of the two syringe pumps, (Supplementary Information Table S1), beads with different diameter (D) were formed: D_2=804 ± 57µm, D_3 = 488 ± 57µm, D_4 = 309 ± 65µm.

Fabrication of Polymeric Foams

PDMS prepolymer solutions were prepared with monomer: curing agent ratios of 10:1 or 5:1 w:w, and degassed in vacuum for few minutes. Calcium alginate beads of each type and the PDMS solution were mixed into a small plastic container of cylindrical shape under vigorous stirring for 1h in order to distribute homogeneously the prepolymer in the whole volume of the beads-filled container. Then, the solution was stored in ambient conditions, favoring the close packing of the beads into the solution due to gravitational forces. After the PDMS curing at room temperature overnight, the samples were extracted from the container and put under low vacuum and temperature of 70 °C for 2h. In this way the beads were forced to dehydrate rapidly, reducing their dimensions. The dry beads were extracted from the cured PDMS matrix after placing the system under a water flow; the pressure exerted by water forces the beads to be mechanically expelled from the PDMS.

Samples Characterization

Optical microscopy studies on the beads and the fabricated foams were conducted by means of a stereo microscope (LEICA S8APO) and an optical microscope (Olympus BX51). The reduction of the size of the beads during dehydration was screened in air, (temperature: 24°C, relative humidity: 60%) upon acquisition of microscope images at defined time intervals. The mean diameter of the beads was calculated by analyzing a set of 80 beads for each type. Scanning electron microscopy (SEM) images and Energy-dispersive X-ray (EDX) spectroscopy were performed by using a Jeol JSM-6490LA variable pressure scanning electron microscope, operated in low vacuum mode (30 Pa) at 10 kV.

Three dimensional images of the foams functionalized with gold NPs were acquired by using a Nikon confocal microscope (Nikon Optical Co., Ltd., Tokyo, Japan) in reflection mode, (excitation wavelength λ_{ex}=488nm, and reflection at λ_{ref}=482nm).

Measurements of apparent water contact angles (APCA) were carried out with a contact angle goniometer (KSVCAM200, Kruss, Germany), using distilled water drops of 5µL. The mean APCAs were calculated based on 5 different measurements for each sample.

Results and discussion

The hydrogel templates for the fabrication of the foams are composed by calcium alginate beads. Alginates are block

copolymers of linear unbranched polysaccharides deriving from marine algae, composed of α-L-guluronic acid (G) and β-D-mannuronic acid (M) proportions[30,31]. For the formation of the beads we start from an aqueous solution of sodium alginate that gets inserted dropwise into a calcium chloride one. Crosslinking of sodium alginate drops is initiated by polyvalent cations, like calcium, forming water insoluble calcium alginate beads[32]. In form of beads, calcium alginate has been widely used to encapsulate both inorganic particles and biomaterials, including proteins and cells[23]. Alginate is also used for the production or encapsulation of NPs, including noble or heavy metals [30, 33-35, 22] or iron oxide [36, 37].

As shown in Fig. 1, the shape of the formed calcium alginate beads depends on their fabrication method. In fact, beads with diameter D_1 of 1.56 ± 0.06 mm are prepared by dropwise addition of sodium alginate aqueous solution in the calcium chloride one and they have a perfect spherical shape. On the other hand, smaller beads (diameters: D_2=804 ± 57μm, D_3 = 488 ± 57μm, D_4 = 309 ± 65μm) are generated by the T-junction fluidic system based on the use of the oil continuous phase to create sodium alginate micro-drops (Supplementary Information Fig. S1). These particles exhibit a teardrop shape that is strictly related to the slow transit of the droplets across the oil-water interface [29]. Despite this fact, the latter method allows us to produce microbeads with controlled size compared to other methods [38-41]. In order to minimize the tip size of the beads, sodium alginate aqueous solutions of different concentrations were tested, revealing that the beads formed by 7%wt of sodium alginate in water have a shape similar to the spherical one (Fig. 1b, and Supplementary Information Fig. S2). The calcium alginate beads have a porous structure and contain a certain amount of water that is released when the beads are stored in ambient conditions (Fig. 1c). This results in a significant volume reduction, of about 95%, independently from the initial beads size, as also confirmed by other studies [28]. Furthermore, the shrinking rate in ambient conditions is similar for all beads' dimensions [28], with 25±1 μm/min, 18 ±1μm/min, 21±1 μm/min and 21±3 μm/min for D_1, D_2, D_3, and D_4 beads, respectively. Therefore, for the larger beads, a complete dehydration is reached after around 38 min, while as the beads are getting smaller, they dehydrate faster reaching c.a. 8 min for D_4 beads. The faster volume reduction for smaller beads is attributed both to the smaller amount of water that they contain and to their larger surface to volume ratio.

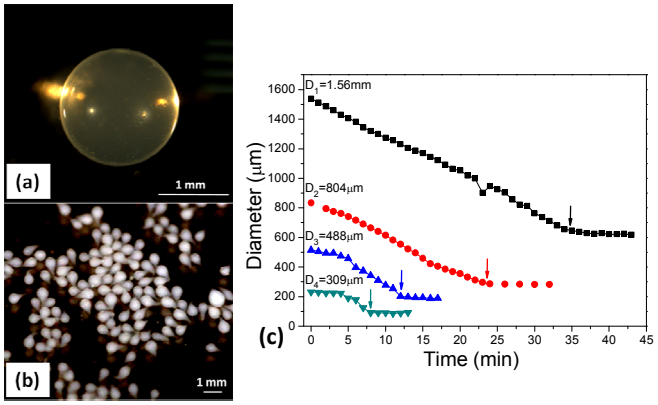

Figure 1. (a), (b) Microscope images of calcium alginate beads of D_1 = 1.56 mm and D_2 = 804 μm respectively. (c) Reduction of the diameter of the beads during time under ambient conditions, for a representative sample of each group. Arrows indicate the time at which the dehydration of the beads is completed.

For the formation of the foams, PDMS prepolymer is poured into vials containing the as prepared beads. The dehydration of the beads proceeds slower than in air, due to the presence of the hydrophobic PDMS matrix, and is long enough to follow its polymerization. The subsequent heating of the cured samples at 70 °C for 2 hours under vacuum terminates the dehydration process of the hydrogel beads. In this way, their diameter is drastically reduced, making thus possible their elimination from the PDMS matrix under the mechanical stress exerted by water flow. Consequently, foams like the ones shown in Fig. 2 are formed, with the size of the pores strictly related to the beads diameter.

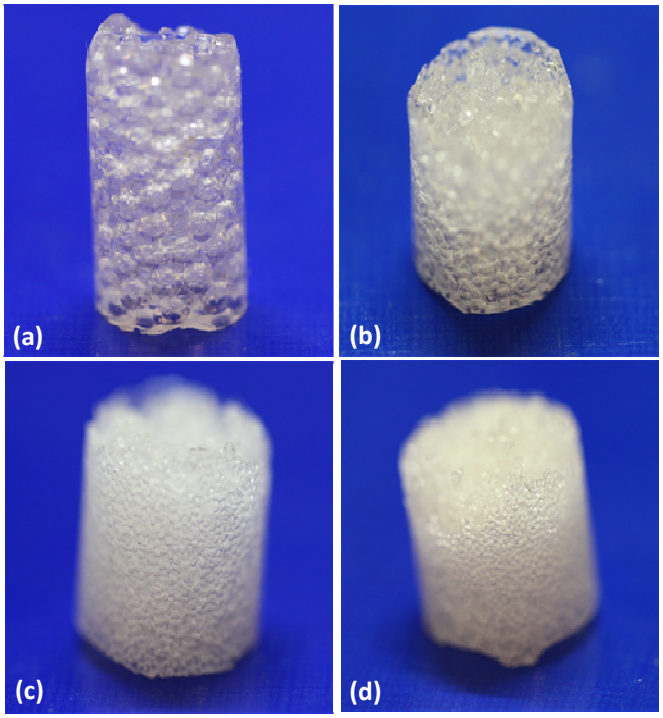

Figure 2. Photographs of PDMS foams fabricated with calcium alginate beads of four different diameters: (a) D_1=1.56 mm, (b) D_2=804 μm, (c) D_3=488 μm and (d) D_4=309 μm. Diameter of the foams c.a. 1 cm.

Optical microscope images of the foams (Fig. 3) reveal that the pores are uniformly distributed in their whole volume while alginate beads residues are not observed. These are indications that the beads remain closely packed in the elastomeric matrix during the polymerization step, while their removal process is effective due to the presence of interconnected pores. This is also confirmed by the SEM investigations (insets Fig. 3a-b), where the existence of open cell units and interconnecting windows is clearly evident. In particular, the dark circular areas visible in the SEM pictures correspond to voids in the cell walls of the PDMS foam related to contact points between two adjacent beads. This can be attributed to

the fact that the contact between the beads remains tight enough in the first minutes of the PDMS polymerization, until a high viscosity of the matrix is reached. The average pore size of the foams, as measured directly from the SEM images, is strictly related to the size of the beads that are utilized for the fabrication of each foam, as shown in Fig.3c. Indeed, in all cases, the average diameter of the pores almost coincides with the diameter of the utilized beads in each case, revealing that by selecting the beads we can directly control the size of the pores of the foams.

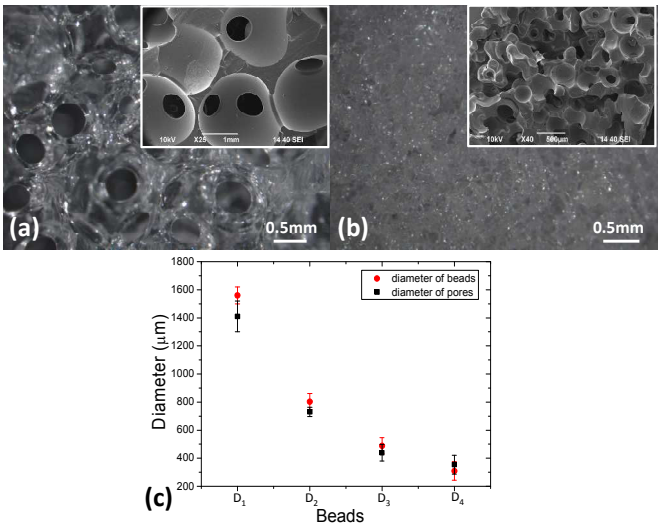

Figure 3. (a), (b) Microscope images of foams fabricated with the D_1=1.56 mm and D_4=309 μm beads respectively. Insets: representative SEM images in each case. (c) Comparison between the mean diameter of the beads and the mean pore size of the corresponding foams.

All fabricated foams are hydrophobic with APCA values higher than the one of the flat PDMS ($APCA_{flat}$: 110°). Most importantly, the APCA increases as the pore size of the foams decreases, reaching almost the superhydrophobic state (144±1°) for foams with the smallest pore size (Fig. 4). This behavior is predicted by the Cassie-Baxter model for hydrophobic surfaces that assumes that when a water drop is placed on a rough or porous substrate it entraps air in the surface gaps, experiencing a "composite" air-solid surface. Therefore, such rough or "composite" surfaces are more hydrophobic than the flat of the same chemical composition, according to the following formula [42]:

$$cos\theta_{CB} = f_{SL}\,(cos\theta_{\gamma} + 1) - 1 \qquad \text{Equation 1}$$

where θ_{CB} is the APCA for each foam, f_{SL} is the fraction of the solid surface in contact with the liquid, and $\theta\gamma$ is the Young's contact angle, i.e., the contact angle of the liquid on the corresponding flat surface with the same chemical characteristics (110° for flat PDMS). By inserting the measured APCA values for the flat PDMS and for the foams, the f_{SL} value for each kind of foam can be extracted. In particular, as the pore size of the foams decreases, the fraction of the solid surface in contact with the liquid drop decreases, indicating the existence of a higher amount of air in contact with the water drop (Fig. 4).

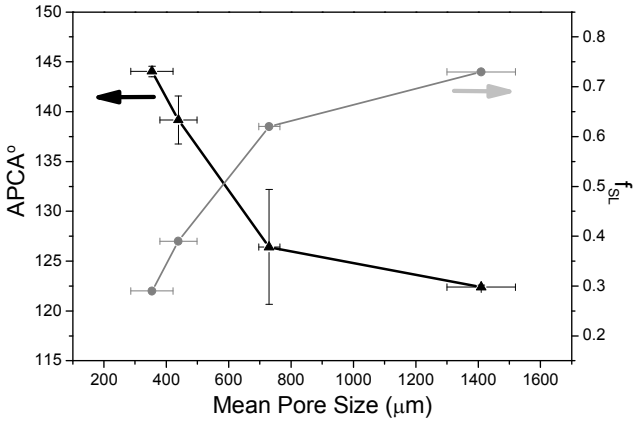

Figure 4. Apparent water contact angle (APCA) and the fraction of the solid surface in contact with the liquid drop (f_{SL}) as a function of the mean pore size of the PDMS foams.

Apart from the precise control of the size of the pores of the foams and of their wettability, another important advantage of the use of calcium alginate beads as templates is the possibility to load them with specific compounds, by simply dispersing the latter in the calcium chloride or in the sodium alginate aqueous solution. Different groups have demonstrated that the beads can entrap metallic ions [30, 33-35, 22, 36, 37] or various types of macromolecules [42, 43] for water cleaning or biomedical applications. Concerning the $AuCl_4^-$ ions, it has been observed that they react with sodium alginate resulting in their chemical reduction and eventually in the formation of gold NPs [44]. However, the higher the concentration of the gold ions the lower the uptake and the reduction capability [32, 45]. In the present case, different concentrations of gold precursor ($HAuCl_4$) dispersed in the aqueous calcium chloride solution are tested, ranging from 0.001% (%wt with respect to the water content) to 0.1%. For concentrations lower that 0.01%, after the formation of the calcium alginate beads, Au^{3+} ions are chemically reduced from the alginate matrix becoming Au^0, thus creating gold NPs into the beads' structure (Supplementary Information Fig. S3). On the other hand, for concentrations higher than 0.01%, the reduction inside the beads is inhibited and the formed calcium alginate beads exhibit a light yellow color, characteristic of the encapsulation of gold precursor solution (Supplementary Information Fig. S4).

Therefore, the as fabricated calcium alginate/gold precursor beads, with concentrations of the latter higher than 0.01%, are used as templates for the formation of polymeric foams with pores decorated with gold NPs, which exhibit a purple color, typical of the formation of gold NPs (Supplementary Information Fig. S5). During the shrinking of the beads in the elastomer matrix, the gold precursor is released, and it is chemically reduced as it comes in contact with the silicon hydride (Si–H) functional groups of PDMS curing agent [46]. In

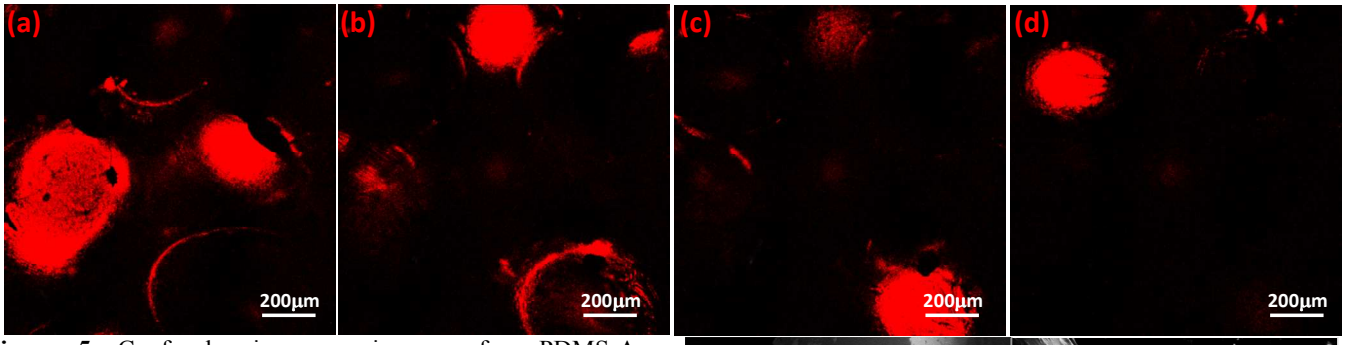

Figure 5. Confocal microscope images of a PDMS-Au composite foam at different focal depths (FD) from the surface of the foams: (a) FD= 385 µm (b) FD= 539 µm, (c) FD= 616 µm and (d) FD= 693 µm.

order to have successful PDMS polymerization and chemical reduction, the concentration of the Si–H groups should be carefully controlled by modifying the ratio between the curing agent and the monomer, the so called η factor. When an excess of curing agent is present in the PDMS prepolymer solution, the Si-H groups not only are reacting with the vinyl groups (Si–$CH{=}CH_2$) of the monomer, initiating thus the polymerization process [46], but are also inducing the chemical reduction of the gold precursor. In order to achieve a well localized functionalization of the cell walls of the foams with NPs, the η factor was defined to be equal to 0.2 (corresponding to a monomer: curing agent ratio of 5:1) while the concentration of $HAuCl_4$ was fixed at 0.1%. For higher concentrations of curing agent and/or gold precursor, the reduction process of gold is enhanced. Therefore, the formation of gold NPs is no more confined into the cavities of the pores, and the localization feature is lost.

The confocal microscope analysis throughout the volume of the foams confirmed the efficiency of the functionalization of the walls of the pores. Choosing a laser wavelength for the measurement, that can be reflected by the gold NPs but is transparent for the elastomeric matrix, it is possible to monitor the formed NPs. As shown in Fig. 5, the laser light from the microscope is highly reflected by the surface of the cells (red regions in Fig. 5) and not by the polymeric matrix (black regions), in the whole depth of the foam, as also shown by the complete scan and the three dimensional reconstruction presented in Supplementary Information (Fig. S6). This proves that the gold NPs are localized exclusively on the surface of the pores. This is further confirmed by a SEM analysis of the morphology of the surface of a pore (Fig. 6). As shown, on the walls of a pore, are present clusters of gold NPs that are localized along the walls of the cavity (Fig. 6a, 6b and 6c). The EDX analysis of the Fig. 6d,e, confirms that the present agglomerates are composed by gold homogeneously distributed on the whole surface studied, while the silicon signal is representative for the PDMS polymer. It should be stressed that the proposed technique can be expanded to countless organic or inorganic substances as long as they exhibit any physicochemical affinity with the polymeric foam.

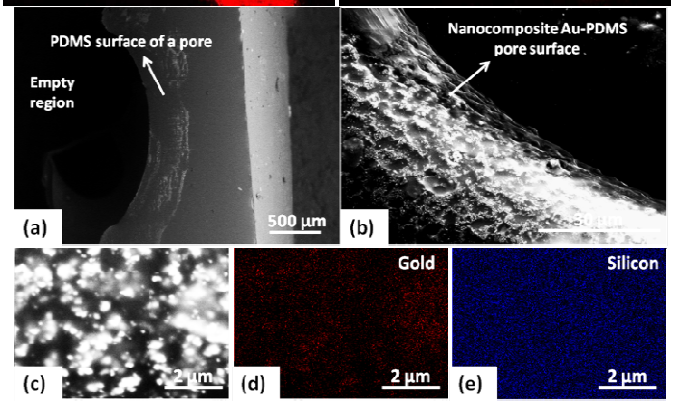

Figure 6. (a), (b), (c) SEM images of a pore surface of the PDMS-Au foam. The bright features correspond to gold NPs and the dark grey zone to the PDMS matrix. (d) and (e) are the EDX maps denoting gold (red) and silicon (blue) composition of the surface imaged at (c).

Conclusions

In this work we present a novel strategy to produce PDMS foams based on the use of closely backed calcium alginate beads as templates. Upon polymer curing, a significant volume reduction of the hydrogel beads makes possible their extraction from the polymer matrix by applying low physical pressure, resulting in the formation of PDMS foams. The hydrogel beads are produced *via* external gelation with a simple fluidics system ensuring a uniform and controlled size of the formed hydrogel particles, and thus of the pores induced into the polymer matrix. Most importantly, the use of hydrogel beads offers the possibility to entrap and release active substances on the cells of the foams functionalizing their surface in a localized manner. As a proof of concept, gold precursor was entrapped in the beads. Upon the formation of the foam, the beads shrink expelling the gold precursor that is subsequently reduced chemically by the PDMS matrix resulting in the formation of gold NPs exclusively localized on the walls of the foams' cells. Such foams can be utilized for the concentration of biological substances in order to induce localized cells growth, for localized reactions, or for localized molecular detection. Due to the presence of gold NPs in defined areas it is possible the entrapment of substances of low concentrations in liquids and also their detection by sensitive techniques (e.g. surface enhanced raman scattering). The proposed method can be used for the fabrication of foams with diverse types of functional

pores, by utilizing different metal precursors or organic substances resulting in the surface functionalization of each single pore of the foam in a different way.

Acknowledgements

The authors thank Mr. Marco Scotto d'Abbusco of Istituto Italiano di Tecnologia for the technical support for confocal microscope analysis.

Notes and references

[a] Center for Biomolecular Nanotechnologies (CBN) @UNILE, Istituto Italiano di Tecnologia (IIT) Via Barsanti, 73010 Arnesano (LE), Lecce, Italy.
[b] Smart Materials Group – Nanophysics, Istituto Italiano di Tecnologia, Via Morego 30, 16163 Genova, Italy.
[c] Nanochemistry, Istituto Italiano di Tecnologia, Via Morego 30, 16163 Genova, Italy.
[*] *E-mail: despina.fragouli@iit.it*

Electronic Supplementary Information (ESI) available: Schematic representation of the T-junction fluidics set-up; table with the experimental parameters used for the formation of beads with different diameters. Figures of: different size and shapes of calcium alginate beads; calcium alginate beads loaded with $HAuCl_4$ gold precursor; calcium alginate beads formed in a calcium chloride solution and in a calcium chloride solution loaded with high concentration of $HAuCl_4$; photograph of an Au-PDMS foam; three dimensional reconstruction by confocal microscopy, of a Au-PDMS foam.

1 S. J. Hollister, *Nature Materials*, 2005, **4**, 518.
2 P. Calcagnile, D. Fragouli, I. S. Bayer, G. C. Anyfantis, L. Martiradonna, P. D. Cozzoli, R. Cingolani, A. Athanassiou, *ACS Nano*, 2012, **6**, 5413.
3 W. Akl, A. Baz, *Journal of Vibration and Control*, 2006, **12**, 1173.
4 D. L. Tomasko, Z. Guo, in *Kirk- Othmer Encyclpoedia of Chemical Technology*, 2007, pp. 1-29.
5 Q. Z. Yan, G. D. Lu, W. F. Zhang, X. H. Ma, C. C. Ge, *Adv. Funct. Mater.*, 2007, **17**, 3355.
6 S. Merlet, C. Marestin, F. Schiets, O. Romeyer, R. M. Merlet, *Macromolecules*, 2007, **40**, 2070.
7 S. Deville, *Materials*, 2010, **3**, 1913.
8 S. Y. Lee, J. H. Oh, J. C. Kim, S. H. Kim, J. W. Choi, *Biomaterials*, 2003, **24**, 5049.
9 M. K. Marei, S. R. Nouh, M. M. Fata, A. M. Faramawy, *Tissue Eng.*,2003, **9**, 713.
10 S. H. Lee, B. S. Kim, S. H. Kim, S. W. Choi,S. I. Jeong, I. K. Kwon, S. W. Kang, J. Nikolovski, D. J. Mooney, Y. K. Han, Y. H. Kim, *J. Biomed. Mater. Res., Part A*, 2003, **66A**, 29.
11 A. Porjazoska, N. Kayaman-Apohan, O. Karal-Yilmaz, M. Cvetkovska, K. Baysal, B. M. Baysal, J. Biomater. *Sci. Polym. Ed.*, 2002, **13**, 1119.
12 S. H. Oh, S. G. Kang, E. S. Kim, S. H. Cho, J. H. Lee, *Biomaterials*, 2003, **24**, 4011.
13 Q. Hou, D. W. Grijpma, J. Feijen, *Biomaterials*, 2003, **24**, 1937.
14 K. J. Lissant, *Journal of colloid and interface science*, 1974, **47**, 416.
15 N. R. Cameron, *Polymer*, 2005, **46**, 1439.
16 C. Guoping, U. Takashi, T. Tetsuya, *Chem. Commun*., 2000, **16**, 1505.
17 J. E. Barralet, L. L. Wallace, A. J. Strain, *Tissue Engineering*, 2003, **9**, 1037.
18 D. J. Mooney, C. L. Mazzoni, C. Breuer, K. McNamara, D. Hern, J. P. Vacanti, R. Langer, *Biomaterials*, 1996, **17**, 115.
19 N. Bhardwaj, S. C. Kundu, *Biotechnology Advances*, 2010, **28**, 327.
20 M. N. Lee, A. Mohraz, *Adv. Mater.*, 2010, **22**, 4836.
21 L. J. Lee, C. Zeng, X. Cao, X. Han, J. Shen, G. Xu, *Composites Science and Technology*, 2005, **65**, 2344.
22 K.- S. Huang, T.- H. Lai, Y.- C. Lin, *Lab Chip*, 2006, **6**, 954.
23 C. H. Goh, P. W. S. Heng, L. W. Chan, *Carbohydr. Polym*, 2012, **88**, 1.
24 M. J. Fiedler, Creating PhD Thesis, University of Washington, 2012.
25 J. T. Delaney, Jr., A. R. Liberski, J. Perelaerbc, U. S. Schubert, *Soft Matter*, 2010, **6**, 866.
26 A. A. Tomei, F. Boschetti, F. Gervaso, M. A. Swartz, *Biotechnology and Bioengineering*, 2009, **103**, 217.
27 M. K. Phull, T. Eydmann , J. Roxburgh, J. R. Sharpe, D. J. Lawrence-Watt , G. Phillips, Y. Martin, *J Mater Sci: Mater Med*, 2012, **24**, 461.
28 H. Hirama,T. Kambe, K. Aketagawa, T. Ota, H. Moriguchi, T. Torii, *Langmuir*, 2013, **29**, 519.
29 L. Capretto, S. Mazzitelli, C. Balestra, A. Tosi, C. Nastruzzi, *Lab Chip*, 2008, **8**, 617.
30 T. A. Davis, B. Voleskya, A. Mucci, *Water Research*, 2003, **37**, 4311.
31 Y. Cheng, X. Luo, G. F. Paynebc, G. W. Rubloff, *J. Mater. Chem.*, 2012, **22**, 7659.
32 W. R. Gombotz, S. F. Wee, *Advanced Drug Delivery Reviews*, 1998, **31**, 267.
33 R. Brayner, M.-J.Vaulay, F. Fiévet, T.Coradin, *Chem. Mater.* 2007, **19**, 1190.
34 Z. Schnepp, S. R. Hall, M. J. Hollamby, S. Mann, E. Kroll, F. M. Winnik, *Chem. Mater.*, 1996, **8**, 1594.
35 E. Kroll, F. M. Winnik, *Chem. Mater.*, 1996, **8**, 1594.
36 R. Naik, U. Senaratne, N. Powell, E. C. Buc, G. M. Tsoi, V. M. Naik, P. P. Vaishnava, L. E. Wenger, *Journal of Appl. Physics*, 2005, **97**, 10.
37 G. Coppi, V. Iannuccelli, M. T. Bernabei and R. Cameroni, *Int. J. Pharm.*, 2002, **242**, 263.
38 S. C. Chen, Y. C. Wu, F. L. Mi, Y. H. Lin, L. C. Yu and H. W. Sung, *J. Controlled Release*, 2004, **96**, 285.
39 L. W. Chan, H. Y. Lee and P. W. S. Heng, *Int. J. Pharm*., 2002, **242**, 259.
40 J. O. You, S. B. Park, H. Y. Park, S. Haam, C. H. Chung and W. S. Kim, *J. Microencapsulation*, 2001, **18**, 521.
41 Y. Hu, O. Wang, J. Wang, J. Zhu, H. Wang, Y. Yang, *Biomicrofluidics*, 2012, **6**, 1.
42 A. B. D. Cassie, S. Baxter, *T Faraday Soc*, 1944, **40**, 546.
43 I. Liakos, L. Rizzello, I. S. Bayer, P. P. Pompa, R. Cingolani, A. Athanassiou, *Carbohydrate Polymers*, 2013, **92**, 176.
44 V. Jaouen, R. Brayner, D. Lantiat, N. Steunou, T. Coradin, *Nanotechnology*, 2010, **21**, 181605.
45 K.-M. Khoo, Y.-P. Ting, *Biochemical Engineering Journal*, 2001, **8**, 51.
46 Q. Zhang, J.-J. Xu, Y. Liu, H.-Y. Chen, *Lab Chip*, 2008, **8**, 352.
47 E. Torres, Y. N. Mata, M. L. Blázquez, J. A. Muñoz, F. González, and A. Ballester, *Langmuir,* 2005, **21**, 7951.

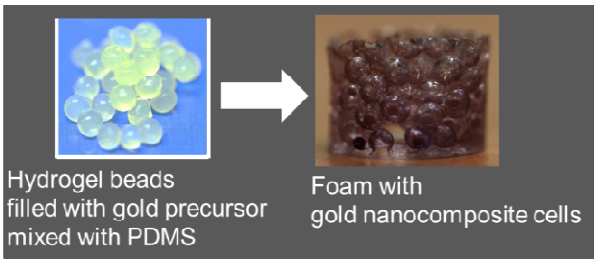

Elastomeric foams with controlled cells size and composition are formed by using calcium alginate hydrogel beads as templates.